ECS Transactions, 3 (20) 7-15 (2007)
10.1149/1.2721509, copyright The Electrochemical Society

Voltammetric Characterization of $[ReO]^{3+}$ Containing Complexes

M.F. Cerdá[a1], C. Kremer[b], A.M. Castro Luna[c], E. Méndez[a]

[a] Laboratorio de Biomateriales, Facultad de Ciencias, 11400 Montevideo, URUGUAY
[b] Cátedra de Química Inorgánica, Facultad de Química, 11800, Montevideo, URUGUAY
[c] INIFTA, Universidad Nacional de la Plata, 1900 La Plata, ARGENTINA

In the present work, the voltammetric profiles of Au-*pc* in 1 mM solutions of $K[Re^{V}OCl_2(L)]$ (L = dianions of H_2hida or H_2eida; hida, n-(2,6-dimethylphenyl carbamoylmethyl)imino diacetic acid, and eida, 2,6-diethyl ida) complexes were evaluated. The obtained electrochemical response was the result of the contributions coming from the $[ReO]^{3+}$ *core* (E_{pa} at ca. 0.2 V vs. $Ag/AgNO_3$) and the carboxylic group of the ligand. There where also observed redox contributions ascribed to the presence of perrhenate coming from the decomposition of the complex with the lost of ligands, in agreement with the low stability of the studied complexes.

Introduction

The use of technetium and rhenium complexes in diagnostic imaging and therapy is still increasing (1-4). Among them, ^{99m}Tc-hida (H_2hida = n-(2,6-dimethylphenyl carbamoyl methyl) imino diacetic acid) was the first Tc radiopharmaceutical designed to replace ^{131}I agents for liver imaging (5-8). During the chemical studies of these complexes, different structures and even different oxidation states for the metal ion were proposed (9-14).

Both the oxidation state and the redox stability in aqueous solution, play an important role in the biodistribution, uptake and elimination of a radiopharmaceutical agent (15), determining its *in vivo* behavior. Hence, the study of the redox stability and the electrochemical behavior become a relevant feature to evaluate the relationship between structure and chemical reactivity.

In this work, the redox behavior of Re(V)-hida and eida (H_2eida = n-(2,6-diethyl phenyl carbamoyl methyl) imino diacetic acid) compounds was evaluated. Re has a stable isotope and allows the manipulation of higher amounts of substance; as a consequence, it is widely used to elucidate physical and chemical properties of such complexes.

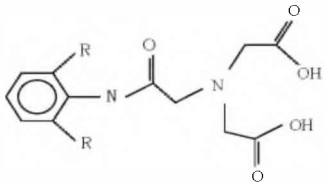

Figure 1. Schematic representation of the ligands; R = CH_3- (H_2hida), CH_3CH_2- (H_2eida)

[1] Corresponding author: María Fernanda Cerdá, fcerda@fcien.edu.uy
(+598 2) 525 0800, fax (+598 2) 525 0895

Downloaded on 2019-08-23 to IP 163.10.34.204 address. Redistribution subject to ECS terms of use (see ecsdl.org/site/terms_use) unless CC License in place (see abstract).

Moreover, and considering the hardness of the carboxylate ligands with respect to the $[ReO]^{3+}$ *core*, it is possible to predict some instability of the complexes. In this situation, lost of ligands and further oxidation of the metallic *core* to perrhenate would also be detected. For this reason, ReO_4^- solutions were also analyzed in order to facilitate the assessment of the observed redox signals in the voltammetric profiles of Au in the complexes solutions.

Experimental section

Complexes were synthesized as previously reported (9), by a ligand exchange route on the precursor $[ReOCl_3(PPh_3)_2]$ (PPh_3 = triphenylphosphine). All chemicals were analytical grade or better. Taking into account the low solubility of the complexes in water, the studies were performed in methanol as solvent.

Working solutions were 1 mM of the free ligands in an aqueous solution of the supporting electrolyte or 1mM of the complexes in methanol.

The supporting electrolyte was 0.04 M $LiClO_4$ in methanol or aqueous 0.04 M $LiClO_4$ (pH = 7.5, Millipore-MilliQ* water, 18.2 MΩ). All potentials in the text are referred to the electrode $Ag/AgNO_3$ 0.1 M in the supporting electrolyte (0.82 V vs. NHE). The working electrode was a wire of polycrystalline Au-*pc* (0.16 cm^2 geometric area) and the counter electrode a Pt sheet (4 cm^2). The working electrode was polished with fine alumina powder (0.1 down to 0.05 μm), sonicated in ultrapure water, immersed in a hot HNO_3 + H_2SO_4 mixture, and thoroughly rinsed with Millipore-MilliQ* water. To check the reproducibility and cleanness of the surface, a stabilized voltammogram of the Au-*pc* electrode in aqueous 1 M sulfuric acid run from 0.23 to 1.67 V-RHE at v = 0.10 V s^{-1} was recorded before each experiment. A well-defined O-electrosorption profile and the width of the double-layer region were taken as purity criteria of the electrode–electrolytic solution interface.

Different potential routines were applied, at potential scan rates v laying in the range 0.005 $Vs^{-1} \leq v \leq$ 0.2 Vs^{-1}, including progressive increases in the upper potential limit E_a at a fixed lower potential value E_c or vice versa. The lower redox states were achieved by holding the potential at -2.0 V, and the resulting species were analyzed through the voltammetric profile obtained in the following positive-going potential scan.

Results and discussion

Characterization of the ligands

The voltammetric profile of Au-*pc* in 1mM H_2hida and H_2ehida solution recorded at 0.1 Vs^{-1} (Table I, Figure 2) showed the presence of different anodic and cathodic contributions. Among them, those anodic contributions labeled **II**, **III** and **IV** were assigned to the behavior of the Au-*pc* in the aqueous supporting electrolyte.

TABLE I. Redox contributions assigned to Au-*pc* in the supporting electrolyte in water, pH = 7.5

Peak label	Epa - V vs. $Ag/AgNO_3$	Epc - V vs. $Ag/AgNO_3$
II	ca. 0.2	
II	0.48	0.13
IV	0.61	

The profile also showed the presence of some contributions assigned to redox processes originated in the ligand, as contribution **I**, with an E_{pa} = 0.03 / 0.10 V (H_2eida

Downloaded on 2019-08-23 to IP 163.10.34.204 address. Redistribution subject to ECS terms of use (see ecsdl.org/site/terms_use) unless CC License in place (see abstract).

or H_2hida respectively) and its counter cathodic peak at E_{pc} = -0.09 V. The contribution **V** is located at E_{pa} = -0.86 / -0.97 V (H_2eida or H_2hida respectively) and the related E_{pc} = -1.35 / -1.37 V.

Moreover, anodic current peak **I** recorded at different *v* showed a linear adjust between i_{pa} and *v*, and the ratio i_{pc}/i_{pa} was lower than 1 (cathodic contribution not noticeable at low *v* and increasing with *v*). Also E_{pa} changed linearly with *v*; the peak potential value increased with *v* for $v \leq 0.08$ Vs^{-1}. Thus, the process associated to peak **I** involved an adsorbed species that could follow an EC process, with slow transfer of the electron (16).

The process could be assigned to the oxidation of the adsorbed carboxylate group to give CO_2, overlapped to the early stages of the O-electro oxidation (17). Then, it would be possible to propose that a competition between water and carboxylate for active sites takes place at the electrode surface, as already observed in amino acid containing solutions (18). Depending on *v*, the oxidation of the carboxylate group takes place faster than O-electrosorption, and this could explain the changes in the tendency of the graphic representation between E_{pa} and *v* (see Figure 3).

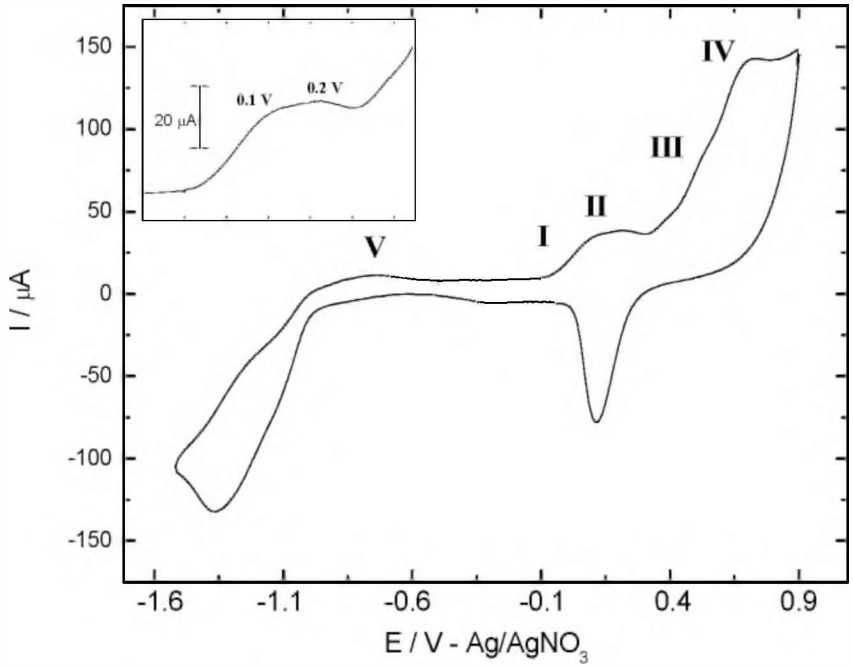

Figure 2. Voltammetric profile of Au-*pc* in 1 mM H_2hida in 0.04 M $LiClO_4$ in aqueous solution, pH = 7.5, *v* = 0.1 Vs^{-1}. Contributions **I** and **II** showed in detail (inset).

Downloaded on 2019-08-23 to IP 163.10.34.204 address. Redistribution subject to ECS terms of use (see ecsdl.org/site/terms_use) unless CC License in place (see abstract).

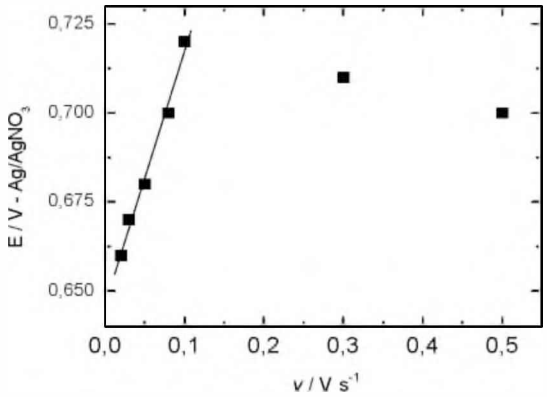

Figure 3. Graphic representation of the E_{pa} corresponding to anodic contribution **I** as a function of *v*, for Au-*pc* in 1 mM H_2hida solution.

With respect to contribution **V**, the cathodic peak showed a linear relationship between the intensity of the current peak and $v^{1/2}$, showing the diffusion of the electroactive species towards the electrode surface. The ratio i_{pa}/i_{pc} was lower than 1, and the value increased with *v* to reach 1 at high *v*. E_{pc} changed following a linear adjustment with ln *v*, with a slope = 0.034 V decade^{-1} in accordance with an electron transfer controlled process (16).

Summarizing, and taking into account that reduction process associated to contribution **V** occurs at $E < E_{pzc}$ of Au-*pc* (E_{pzc} = -0.90 V vs. $Ag/AgNO_3$), and anodic process associated to peak **I** takes place at $E > E_{pzc}$, it can be concluded that cathodic peak **V** involves the reduction of carboxylate to aldehyde. This process is reverted in the anodic scan and when the applied potential E is more positive than E_{pzc} the species is oxidatively desorbed as CO_2 at 0.03 / 0.10 V (H_2eida and H_2hida, respectively).

Based on the above discussion, the following mechanism can be proposed for the redox reactions involving the ligands (19):

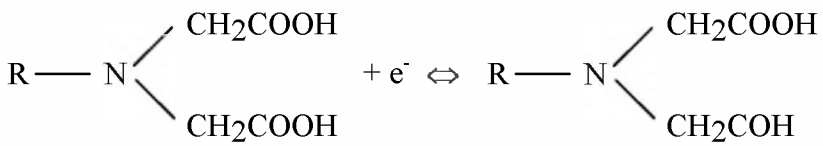

occurs at potential contributions labeled **V**

while at anodic peak named **I**:

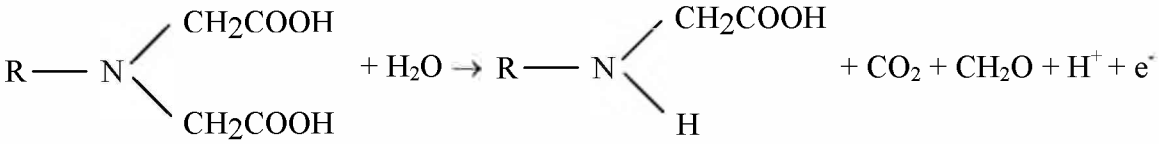

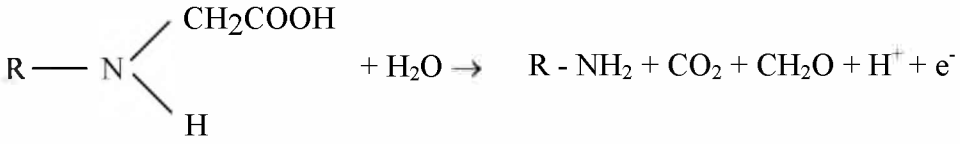

Downloaded on 2019-08-23 to IP 163.10.34.204 address. Redistribution subject to ECS terms of use (see ecsdl.org/site/terms_use) unless CC License in place (see abstract).

Characterization of the complexes

The voltammetric profile of Au-*pc* in 1 mM solutions of the complexes showed the presence of the contributions arising from the free ligand in the supporting electrolyte (Figure 4). It also showed the presence of some new contributions that could be assigned to redox processes centered in the metallic *core* $[ReO]^{3+}$ (Table II).

TABLE II. Redox contributions assigned to redox processes centered in the Re(V) *core* for the hida complex.

Epa (V) vs. $Ag/AgNO_3$	Epc (V) vs. $Ag/AgNO_3$	couple
-0.62		ReO_2 / ReO
-0.48	-0.56 / -0.54	ReO_2 / $[Re(III)O]^+$
-0.46		$[Re(III)O]^+$ / ReO
-0.26	-0.31	ReO_4^- / ReO_2
-0.18		
0.22	ca. 0.1	Re(V) / Re(VI) without decomposition of the complex

Most of the detected contributions were assigned to species coming from the decomposition of the metallic center with lost of the ligands. This fact is in line with the low stability of these complexes, as observed in previous studies (9). Only the anodic contribution at ca. 0.2 V could be attributed to the oxidation of Re(V) to Re(VI) without the lost of the ligands. This contribution was previously detected at the same potential in other Re(V) oxo complexes (18,20,21).

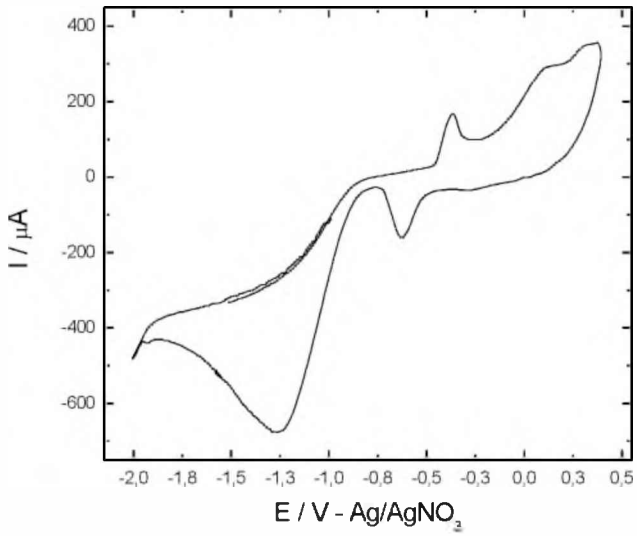

Figure 4. Voltammetric profile of Au-*pc* in 1 mM $K[ReOCl_2(hida)]$ in $LiClO_4$ 0.04 M in methanol, $v = 0.1$ Vs^{-1}.

Downloaded on 2019-08-23 to IP 163.10.34.204 address. Redistribution subject to ECS terms of use (see ecsdl.org/site/terms_use) unless CC License in place (see abstract).

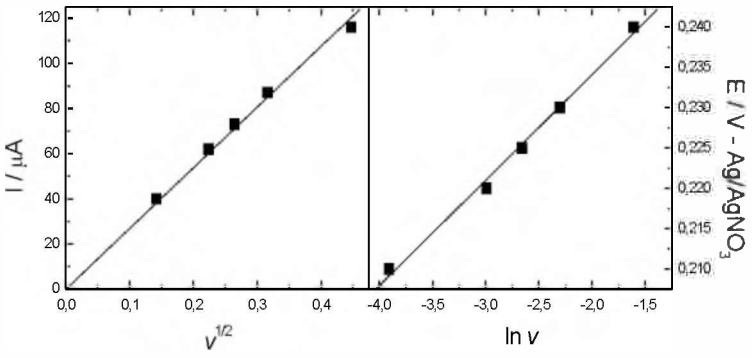

Figure 5. Scan rate dependant parameters of the peak related to oxidation of Re(V) to Re(VI): (a) between I_{pa} and $v^{1/2}$ (b) between E_a and ln v.

The cathodic related counter peak was detected at E_c = 0.10 V. The ratio i_{pc}/i_{pa} was lower than 1. Moreover, i_{pa} showed a linear relationship with $v^{1/2}$ (according to a process where the electroactive species diffuses onto the electrode) and E_{pa} varied linearly with ln v (slope = 0.013 V decade^{-1}) (Figure 5), in line with a process where the electron transfer is slow. The anodic process was assigned to:

$$[Re^{V}OCl_2(L)]^- \rightarrow [Re^{VI}OCl_2(L)] + e$$

with L = dianionic deprotonated form of hida or eida

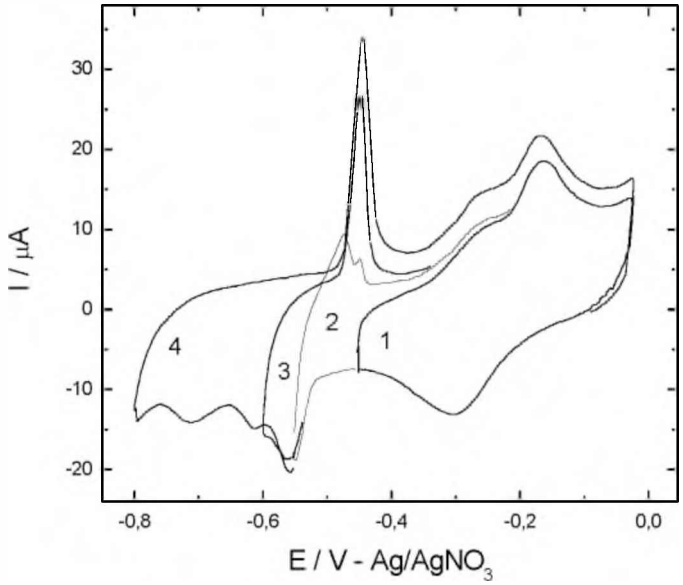

Figure 6. Profile of Au-*pc* in 1 mM K[$ReOCl_2$(hida)] in 0.04 M LiClO4 in methanol, v = 0.1 Vs^{-1}.

As mentioned above, these complexes are very unstable, and decompose very fast to yield the free ligands and ReO_4^- (Figure 6). For this reason, and in order to allow a more adequate assignation of the observed redox signals, voltammetric profiles of perrhenate solutions were also evaluated (Figure 7). Thus, and taking also into account previously

Downloaded on 2019-08-23 to IP 163.10.34.204 address. Redistribution subject to ECS terms of use (see ecsdl.org/site/terms_use) unless CC License in place (see abstract).

reported results (22,23), peaks were attributed to species with different Re oxidation states as described in Table II.

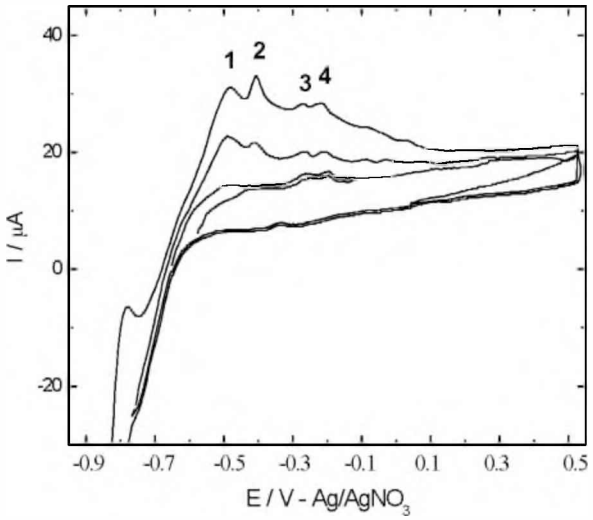

Figure 7. Profile of Au-*pc* in 1 mM solution of ReO_4^- in 0.5 M H_2SO_4, v = 0.1 Vs^{-1}.

Anodic contribution at -0.46 V (related to ReO_2 formation) was present in the profile even in the first cycle of potential scan, and the intensity of its current peaks grow up in the following potential scans. After some cycles, it appeared separate in two different contributions, at:

$$[Re^{III}O]^+ \rightarrow ReO_2 \qquad E_a = -0.46 \text{ V}$$

$$ReO \rightarrow [Re^{III}O]^+ \qquad E_a = -0.48 \text{ V}$$

As can be observed in Figure 6, when a lower potential E_c = -0.62 V is reached (for an upper potential E_a = 0.0 V), the following potential scan towards the positive potentials direction showed a marked increase in the E_a at ca. -0.5 V. The explanation could be found in the formation of ReO from rhenium (IV) dioxide at -0.62 V, with the subsequent formation of ReO_2 when the direction of the potential scan is reverted.

Moreover, when the potential was maintained for 3 minutes at E = -2.0 V, then switched at a lower potential E_c = -0.8 V and reaching an upper potential E_a = 0.0 V, some changes in the profile were observed:

- an increase in the intensity of the current peak at E_c = -0.62 V ($ReO_2 \rightarrow ReO$)
- an increase in the intensity of the anodic peak at ca. -0.5 V ($ReO \rightarrow ReO_2$)

That means, when applying very negative potentials it is possible to reduce directly the Re(IV) dioxide to Re(II) oxide, without the detection of the soluble Re(III) species [22,23].

Finally, anodic contributions at -0.26 V and -0.17 V were assigned to perrhenate formation from ReO_2; this process took place at different applied potential depending on the layers of adsorbed rhenium dioxide (22). Oxidation from bidimensional monolayers happened at -0.26 V, and from dioxide multilayers were observed at -0.17 V.

It was interesting to asses the formation of soluble species of $[Re^{III}O]^+$, a process that was postulated in previous works (22,23) performed from perrhenate solutions. The

Downloaded on 2019-08-23 to IP 163.10.34.204 address. Redistribution subject to ECS terms of use (see ecsdl.org/site/terms_use) unless CC License in place (see abstract).

studied ida-derivatives complexes contained the *core* $[Re^{V}O]^{3+}$ and for them, the exchange of electrons without structural modifications yields the $[Re^{III}O]^{+}$ specie.

The study of perrhenate solutions allowed confirming some of the hypothesis mentioned above. As can be observed in figure 7, the presence of anodic peaks **1** and **2** (at -0.50 V and -0.43 V respectively) depended on the applied potential lower limit. In particular, peak **2** increased when a lower potential E_c = -0.7 V was reached. As was explained before, cathodic contribution at ca. -0.7 V could be attributed to the reduction of ReO_2 to ReO, and anodic peak **2** involved the opposite process. Other contributions, as anodic **3** and **4**, were assigned to the formation of perrhenate from ReO_2, as in the case of the complexes.

It is important to remark that contributions that could involve the presence of soluble $[Re^{III}O]^{+}$ are harder to detect in case of working with perrhenate solutions. Therefore, to detect its presence using Re complexes containing a structural *core* **{**ReO**}** gain greater importance.

Conclusions

The voltammetric profile of the complexes showed the presence of many redox contributions, mostly belonging to the ligands. Among them, an important cathodic peak at -1.35 V was attributed to the reduction of the carboxylate group of the ida-derivatives, and the anodic contribution at around 0.1 V was assigned to the evolution of CO_2 from the carboxylate.

The presence of a couple at ca. 0.2 V was attributed to the exchange of one electron from the Re(V) *core*; this couple was found at the same potential as for other Re(V) complexes.

The instability of the studied complexes with lost of ligands could explain the formation of ReO_4^- due to oxidation of the *core*. As a consequence, several redox contributions were detected in the voltammetric profile, related to redox processes involving the perrhenate.

Acknowledgments

Financial support from CSIC – Uruguay is acknowledged. MFC, EM and CK are researchers from PEDECIBA Uruguay. AMCL is a researcher from CIC Argentina.

References

1. D.E. Reichert, J.S. Lewis, C.J. Anderson, *Coord. Chem. Rev.*, **184**, 3 (1999).
2. S.S. Jurisson, J.D. Lydon, *Chem. Rev.*, **99,** 2205 (1999).
3. Z. Guo, P.J. Sadler, Adv. *Inorg. Chem.*, **49**, 183 (1999).
4. S. Liu, D.S. Edwards, *Chem. Rev.*, **99** 2235 (1999).
5. K. Schwochau, *Technetium*, Wiley-VCH Verlag GmbH, Weinheim (2000).
6. J.R. Dilworth, S.J. Parrott, *Chem.Soc.Rev.*, **27,** 43 (1998).
7. M.J. Abrams, B.A. Murrer, *Science*, **261,** 725 (1993).
8. C.E. Housecroft, *Coord.Chem.Rev.*, **169,** 187 (1998).
9. M.F. Cerdá, C. Kremer, E. Kremer, A. León, in *Technetium, Rhenium and Other Metals in Chemistry and Nuclear Medicine 5*, M. Nicolini M, U. Mazzi, Editors, p. 277, SG Editoriali, Padova, Italy, (1999).
10. M.D. Loberg, A.T. Fields, *Int.J.Appl.Rad.Isot.*, **29**, 167 (1978).

Downloaded on 2019-08-23 to IP 163.10.34.204 address. Redistribution subject to ECS terms of use (see ecsdl.org/site/terms_use) unless CC License in place (see abstract).

11. C.E. Costello, J.W. Brodack, A.G. Jones, A. Davison, D.L. Johnson, S. Kasina, A.R. Fritzberg, *J.Nucl.Med.*, **24,** 353 (1983).
12. F. Callery, *J.Nucl.Med.*, **19**, 962 (1976).
13. M.D. Loberg, J.T. Cooper, *J.Nucl.Med.*, **17**, 633 (1976).
14. M.W. Billinghurst, K. Eckert, K. Mang'era, *Appl.Rad.Isot.*, **61**, 1150 (2004).
15. M.F. Cerdá, E. Méndez, G. Obal, J.S. Gancheff, C. Kremer, A.M. Castro Luna, *J.Inorg.Biochem.*, **98**, 238 (2004).
16. C.H. Hamann, A. Hamnett, W. Vielstich, *Electrochemistry*, Wiley-VCH Verlag GmbH, Weinheim (1998).
17. J. Silva-Chong, E. Méndez, J.L. Rodríguez, M.C. Arévalo, E. Pastor, *Electrochim. Acta*, **47**, 1441 (2002).
18. M.F. Cerdá, E. Méndez, L. Malacrida, C.F. Zinola, C. Melián, M.E. Martins, A.M. Castro Luna, C. Kremer, *J. Colloid Interface Sci.*, **249,** 366 (2002).
19. J.W. Johnson, H.W. Jiang, S.B. Hanna, J. James, *J.Electrochem.Soc*, **119**, 575 (1972).
20. M.F. Cerdá, E. Méndez, J.S. Gancheff, C. Kremer, A.M. Castro Luna, *Inorg. Chem. Comm*, **6,** 189 (2003).
21. M.F. Cerdá, G. Obal, E. Méndez, C.F. Zinola, C. Kremer, M.E. Martins, A.M. Castro Luna, *J.Colloid Interface Sci.*, **236,** 104 (2001).
22. E. Méndez, M.F. Cerdá, A.M. Castro Luna, C.F. Zinola, C. Kremer, M.E. Martins, *J.Colloid Interface Sci.*, **263**, 119 (2003).
23. E. Méndez, M.F. Cerdá, A.M. Castro Luna, C.F. Zinola, M.E. Martins, *React.Kinetic Catal. Letters.*, 77, 371 (2002).

Downloaded on 2019-08-23 to IP 163.10.34.204 address. Redistribution subject to ECS terms of use (see ecsdl.org/site/terms_use) unless CC License in place (see abstract).